Permissible symmetries of multi-domain configurations in perovskite ferroelectric crystals

Jiří Erhart[a)] and Wenwu Cao[b)]
Department of Physics and Materials Science, City University of Hong Kong, 83 Tat Chee Avenue, Kowloon, Hong Kong, People's Republic of China

(Received 21 May 2003; accepted 18 June 2003)

Permissible symmetries of multi-domain structures are analyzed in the $m\bar{3}m \rightarrow 3m$, $m\bar{3}m \rightarrow 4mm$ and $m\bar{3}m \rightarrow mm2$ ferroelectric species. Domain structures produced by the application of external electric and/or mechanical fields that allow for the formation of two-dimensional domain superlattice are described in terms of effective group symmetry. Based on our analysis, the most perspective directions for properties enhancement through domain engineering are specified for perovskite ferroelectric crystals having tetragonal, rhombohedral, and orthorhombic symmetries.
 [DOI: 10.1063/1.1599627]

I. INTRODUCTION

One of the most fascinating phenomena associated with structural phase transition is the formation of domain structures. When there is more than one low temperature variant, twinning is unavoidable under natural conditions. Commonly reported twins in ferroelectric systems are 180°, 90°, 60°, and 120° twins. There is also twinning of other angles, such as 109° and 71°, as well as twinnings involve S walls (also called W′ walls).

Many useful ferroelectric materials have the so-called perovskite structure, which contains three types of lattice positions: body center, corners, and face centers in a cubic unit cell. The ferroelectric phases of perovskite materials are often multi-domain systems because of the energy degeneracy of several variants. Many fascinating domain patterns have been observed in them, for example, in tetragonal thin film of $Pb(Zr_xTi_{1-x})O_3$ (PZT),[1] tetragonal $PbTiO_3$,[2] rhombohedral PZT,[3] and $Pb(Zn_{1/3}Nb_{2/3})O_3-PbTiO_3$ (PZN-PT)[4,5] crystals, and in orthorhombic phase $BaTiO_3$[6] and $KNbO_3$[7,8] crystals. In $KNbO_3$, the S-wall and W-wall intersections have also been observed.[7]

Recently, a lot of attention has been paid to the multi-domain structures owing to the discovery of strong piezoelectric property enhancement in the domain-engineered ferroelectric single crystals of relaxor based $Pb(Zr_{1/3}Nb_{2/3})O_3-PbTiO_3$ (PZN-PT) and $Pb(Mg_{1/3}Nb_{2/3})O_3-PbTiO_3$ (PMN-PT). Such single crystals are poled along a nonpolar but high symmetry axis to intentionally produce multi-domain structures, for example, poling along [001] or [011] in the cubic coordinates. These multi-domain crystals show extremely high piezoelectric coefficient $d_{33} \sim 2500$pC/N and electromechanical coupling factor $k_{33} \sim 95\%$.[9] Based on the same principle, enhancement in piezoelectric coefficient has also been reported for normal ferroelectric crystals $BaTiO_3$[10,11] and $KNbO_3$[12] and in solid solutions $(Na_{1/2}Bi_{1/2})TiO_3$-$BaTiO_3$ (NBT-BT)[13] and $PB(Yb_{1/2}Nb_{1/2})O_3$-$PBTiO_3$ (PYN-PT).[14,15]

Since the domain pattern symmetry is quite different from the underlying crystal symmetry, it is natural to ask what kind of symmetry could be produced in a given ferroelectric system. Some preliminary theoretical studies have been performed on the perovskite ferroelectrics for equal[16] and nonequal[17] volume ratio of domains. It was suggested that domain-engineered structures might be classified into two different categories.[16]

TABLE I. Permissible domain wall orientations in $m\bar{3}m \rightarrow 3m$ ferroelectrics. Parameters are defined as follows: $P^{I}=1/\sqrt{3}P_S(111)$, $P^{II}=1/\sqrt{3}P_S(1\bar{1}1)$, $P^{III}=1/\sqrt{3}P_S(\bar{1}11)$, $P^{IV}=1/\sqrt{3}P_S(\bar{1}11)$, $P^{V}=1/\sqrt{3}P_S(\bar{1}11)$, $P^{VI}=1/\sqrt{3}P_S(11\bar{1})$, $P^{VII}=1/\sqrt{3}P_S(111)$, $P^{VIII}=1/\sqrt{3}P_S(11\bar{1})$.

	P^{I}	P^{II}	P^{III}	P^{IV}	P^{V}	P^{VI}	P^{VII}	P^{VIII}
P^{I}	N/A	(010) (101)	(001) (110)	(100) (011)	Any	(010) (101)	(001) (110)	(100) (011)
P^{II}		N/A	(100) $(0\bar{1}1)$	(001) $(\bar{1}10)$	(010) (101)	Any	(100) $(0\bar{1}1)$	(001) $(\bar{1}10)$
P^{III}			N/A	(010) $(\bar{1}01)$	(001) (110)	(100) $(0\bar{1}1)$	Any	(010) $(\bar{1}01)$
P^{IV}				N/A	(100) (011)	(001) $(\bar{1}10)$	(010) $(\bar{1}01)$	Any
P^{V}					N/A	(010) (101)	(001) (110)	(100) (011)
P^{VI}						N/A	(100) $(0\bar{1}1)$	(001) $(\bar{1}10)$
P^{VII}							N/A	(010) $(\bar{1}01)$
P^{VIII}								N/A

[a)]On leave from the Department of Physics and International Center for Piezoelectric Research, Technical University of Liberec, Hálkova 6, CZ-461 17 Liberec 1, Czech Republic.
[b)]Author to whom correspondence should be addressed. On leave from the Department of Mathematics, The Pennsylvania State University, University Park, PA 16802; electronic mail: cao@math.psu.edu

TABLE II. Permissible domain wall orientations in $m\bar{3}m \rightarrow 4mm$ ferroelectrics. Parameters are defined as follows: $P^{\mathrm{I}}=P_S(100)$, $P^{\mathrm{II}}=P_S(010)$, $P^{\mathrm{III}}=P_S(001)$, $P^{\mathrm{IV}}=P_S(\bar{1}00)$, $P^{\mathrm{V}}=P_S(0\bar{1}0)$, $P^{\mathrm{VI}}=P_S(00\bar{1})$.

	P^{I}	P^{II}	P^{III}	P^{IV}	P^{V}	P^{VI}
P^{I}	N/A	$(1\bar{1}0)$ $(\bar{1}10)$	$(1\bar{0}1)$ $(\bar{1}01)$	Any	$(1\bar{1}0)$ $(\bar{1}10)$	$(1\bar{0}1)$ $(\bar{1}01)$
P^{II}		N/A	$(01\bar{1})$ $(0\bar{1}1)$	$(1\bar{1}0)$ $(\bar{1}10)$	Any	$(01\bar{1})$ $(0\bar{1}1)$
P^{III}			N/A	$(1\bar{0}1)$ $(\bar{1}01)$	$(01\bar{1})$ $(0\bar{1}1)$	Any
P^{IV}				N/A	$(1\bar{1}0)$ $(\bar{1}10)$	$(1\bar{0}1)$ $(\bar{1}01)$
P^{V}					N/A	$(01\bar{1})$ $(0\bar{1}1)$
P^{VI}						N/A

TABLE III. Permissible domain wall orientations in $m\bar{3}m \rightarrow mm2$ ferroelectrics. Parameters are defined as follows: $P^{\mathrm{I}}=1/\sqrt{2}P_S(101)$, $P^{\mathrm{II}}=1/\sqrt{2}P_S(\bar{1}01)$, $P^{\mathrm{III}}=1/\sqrt{2}P_S(011)$, $P^{\mathrm{IV}}=1/\sqrt{2}P_S(0\bar{1}1)$, $P^{\mathrm{V}}=1/\sqrt{2}P_S(\bar{1}0\bar{1})$, $P^{\mathrm{VI}}=1/\sqrt{2}P_S(\bar{1}01)$, $P^{\mathrm{VII}}=1/\sqrt{2}P_S(01\bar{1})$, $P^{\mathrm{VIII}}=1/\sqrt{2}P_S(0\bar{1}1)$, $P^{\mathrm{IX}}=1/\sqrt{2}P_S(110)$, $P^{\mathrm{X}}=1/\sqrt{2}P_S(1\bar{1}0)$, $P^{\mathrm{XI}}=1/\sqrt{2}P_S(\bar{1}10)$, $P^{\mathrm{XII}}=1/\sqrt{2}P_S(\bar{1}10)$, $K=Q_{44}/Q_{11}-Q_{12}$.

	P^{I}	P^{II}	P^{III}	P^{IV}	P^{V}	P^{VI}	P^{VII}	P^{VIII}	P^{IX}	P^{X}	P^{XI}	P^{XII}
P^{I}	N/A	(100) (001)	$(\bar{1}10)$ $(11K)$	$(1\bar{1}0)$ $(1\bar{1}K)$	Any	(001) (100)	$(1\bar{1}K)$ $(\bar{1}10)$	$(1\bar{1}\bar{K})$ (110)	$(0\bar{1}1)$ $(K11)$	$(01\bar{1})$ $(K\bar{1}1)$	$(K1\bar{1})$ $(01\bar{1})$	$(K\bar{1}\bar{1})$ (011)
P^{II}		N/A	$(1\bar{1}0)$ $(\bar{1}1K)$	$(\bar{1}\bar{1}0)$ $(\bar{1}1K)$	(001) (100)	Any	$(\bar{1}\bar{1}K)$ (110)	$(\bar{1}\bar{1}\bar{K})$ $(\bar{1}\bar{1}0)$	$(K1\bar{1})$ (011)	$(K\bar{1}\bar{1})$ $(0\bar{1}1)$	(011) $(K1\bar{1})$	$(0\bar{1}\bar{1})$ $(K\bar{1}\bar{1})$
P^{III}			N/A	(010) (001)	$(1\bar{1}K)$ $(\bar{1}10)$	$(\bar{1}\bar{1}K)$ (110)	Any	(001) (010)	$(\bar{1}\bar{0}1)$ $(1K1)$	$(\bar{1}K1)$ (101)	$(1K1)$ $(\bar{1}\bar{0}1)$	$(\bar{1}01)$ $(\bar{1}K1)$
P^{IV}				N/A	$(1\bar{1}K)$ (110)	$(\bar{1}\bar{1}K)$ $(\bar{1}\bar{1}0)$	(001) (010)	Any	$(1K\bar{1})$ (101)	$(\bar{1}\bar{0}1)$ $(\bar{1}K\bar{1})$	(101) $(1K1)$	$(\bar{1}K\bar{1})$ $(\bar{1}\bar{0}1)$
P^{V}					N/A	(100) (001)	$(\bar{1}10)$ $(11K)$	(110) $(1\bar{1}K)$	$(K11)$ $(0\bar{1}1)$	$(K\bar{1}1)$ (011)	$(0\bar{1}1)$ $(K11)$	$(01\bar{1})$ $(K\bar{1}1)$
P^{VI}						N/A	(110) $(\bar{1}1K)$	$(\bar{1}10)$ $(\bar{1}1K)$	(011) $(K11)$	$(0\bar{1}1)$ $(K\bar{1}1)$	$(K1\bar{1})$ (011)	$(K\bar{1}\bar{1})$ $(0\bar{1}1)$
P^{VII}							N/A	(010) (001)	$(1K1)$ $(\bar{1}\bar{0}1)$	$(\bar{1}01)$ $(1\bar{1}K1)$	$(\bar{1}\bar{0}1)$ $(1K1)$	$(\bar{1}K1)$ (101)
P^{VIII}								N/A	(101) $(1K1)$	$(\bar{1}K\bar{1})$ $(\bar{1}\bar{0}1)$	$(1K\bar{1})$ (101)	$(\bar{1}\bar{0}1)$ $(\bar{1}K1)$
P^{IX}									N/A	(010) (100)	Any	(100) (010)
P^{X}										N/A	(100) (010)	Any
P^{XI}											N/A	(010) (100)
P^{XII}												N/A

TABLE IV. Possible intersections of domain walls in $m\bar{3}m \rightarrow 3m$ ferroelectric species. One example for each intersection line is listed here, other equivalent intersection line orientations could be generated on the basis of parent phase symmetry.

Intersection line	(100)	(011)	(111)
Domain walls	(010),(001),(011),$(01\bar{1})$	(100),$(01\bar{1})$	$(1\bar{1}0)$,$(\bar{1}0\bar{1})$,$(01\bar{1})$

TABLE V. Possible intersections of domain walls in $m\bar{3}m \rightarrow 4mm$ ferroelectric species. One example for each intersection line is listed here, other equivalent intersection line orientations could be generated on the basis of parent phase symmetry.

Intersection line	(100)	(111)
Domain walls	(011), $(01\bar{1})$	$(1\bar{1}0)$, $(10\bar{1})$, $(0\bar{1}1)$

(1) domain-geometry engineering, where the space distribution of domains is of primary importance (applications include constructive interference for second harmonic generation); and
(2) domain-average engineering, where the distribution of polar directions is the most important (applications for transducers and actuators using effective high d_{33} coefficient).

An attempt has also been made to find the external fields (electric, mechanical stress) needed to stabilize multi-domain ferroelectric structures.[18] Generally speaking, the effective symmetry for twinned ferroelectric crystals may be lower than that of single-domain crystallographic symmetry as shown in examples[19] but one could also design domain structures with symmetry higher than that of the crystal symmetry. Complete material property tensor components for multi-domain PZN-PT[20] and PMN-PT[21] have been measured based on the assumption of $4mm$ domain pattern symmetry. However, it is shown experimentally that the effective symmetry can be different from that of the $4mm$ symmetry in many domain-engineered samples.[22]

In this article, we report a detailed analysis on possible point group symmetries of multi-domain configurations in perovskite ferroelectrics resulting from $m\bar{3}m \rightarrow 3m$, $m\bar{3}m \rightarrow 4mm$ and $m\bar{3}m \rightarrow mm2$ phase transitions, including domain walls. We have also added constraints of two-dimensional translation symmetry, which provides possible space group symmetries that can be produced using the domain engineering method, or producing domain superlattice.

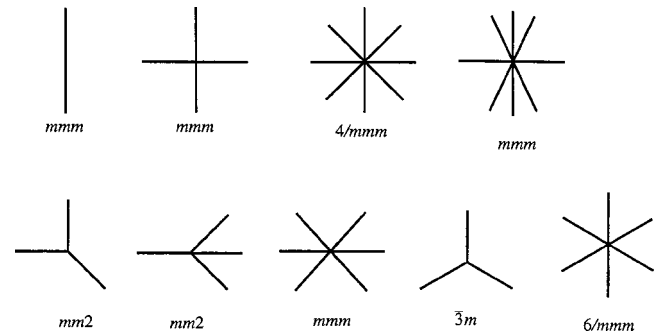

FIG. 1. Domain wall configurations in ferroelectric crystals. Lines denote projections of the domain walls. Domain wall set symmetry is as specified.

II. SYMMETRY ANALYSIS OF DOMAIN STRUCTURES CONTAINING DOMAIN WALLS

Our analysis here differs from that given in Refs. 16 and 17 in which statistical analysis was employed and different domains are allowed to overlap in space. In our analysis here, the orientation of domain walls is taken into consideration and a space is restricted to allow only one domain to exist. In other words, specific domain configurations and their symmetries are given instead of statistical average. For any given crystal symmetry, domain walls can only orient in certain crystallographic directions, which can be derived using the method given in Ref. 23 based on the matching of spontaneous strain at the domain walls. Complete sets of domain wall orientations for $m\bar{3}m \rightarrow 3m$, $m\bar{3}m \rightarrow 4mm$, and $m\bar{3}m \rightarrow mm2$ ferroelectric species are listed in Tables I, II, and III, respectively. Possible intersection lines for different domain wall pairs are calculated as a vector product of the normal vectors (see Tables IV, V, and VI). Possible domain wall sets are derived based on the possibility of domain walls intersecting at the same interface line. Figure 1 shows all domain wall sets and their symmetries. After getting the permissible domain wall orientations (Tables I, II, and III.), which reflect the elastic constraints, polar direction set is added to complete the domain configuration symmetry. For

TABLE VI. Possible intersections of domain walls in $m\bar{3}m \rightarrow mm2$ ferroelectric species. One example for each intersection line is listed here, other equivalent intersection line orientations could be generated on the basis of parent phase symmetry.

Intersection line	(100)	(011)	(111)	$(0K1)$
Domain walls	(010), (001), (011), $(01\bar{1})$	(100), $(01\bar{1})$, $(K11)$, $(K1\bar{1})$	$(1\bar{1}0)$, $(10\bar{1})$, $(01\bar{1})$	(100), $(11\bar{K})$, $(1\bar{1}K)$
Intersection line	$(0K\bar{1})$	$(KK2)$	$(KK\bar{2})$	$(K\bar{K}2)$
Domain walls	(100), $(11K)$, $(1\bar{1}K)$	$(1\bar{1}0)$, $(11K)$	$(1\bar{1}0)$, $(11K)$	(110), $(1\bar{1}K)$
Intersection line	$(1,1,K+1)$	$(\bar{1},1,K+1)$	$(1,\bar{1},K+1)$	$(\bar{1},\bar{1},K+1)$
Domain walls	$(1\bar{1}0)$, $(K1\bar{1})$, $(1K\bar{1})$	(110), $(K11)$, $(1K\bar{1})$	(110), $(K1\bar{1})$, $(1K1)$	$(1\bar{1}0)$, $(K11)$, $(1K1)$
Intersection line	$(1,1,K-1)$	$(\bar{1},1,K-1)$	$(1,\bar{1},K-1)$	$(\bar{1},\bar{1},K-1)$
Domain walls	$(1\bar{1}0)$, $(K\bar{1}1)$, $(1K\bar{1})$	(110), $(K11)$, $(1K\bar{1})$	(110), $(K1\bar{1})$, $(1K1)$	$(1\bar{1}0)$, $(K\bar{1}1)$, $(1K1)$
Intersection line	$(K^2+1,K+1,K-1)$	$(K^2+1,K-1,K+1)$	$(K^2+1,K+1,1-K)$	$(K^2+1,1-K,K+1)$
Domain walls	$(1\bar{1}K)$, $(1K\bar{1})$	$(11\bar{K})$, $(\bar{1}K1)$	$(1\bar{1}K)$, $(1K1)$	$(1\bar{1}K)$, $(1K1)$
Intersection line	$(K^2+1,-K-1,K-1)$	$(K^2+1,-K-1,1-K)$	$(K^2+1,K-1,-K-1)$	$(K^2+1,1-K,-K-1)$
Domain walls	$(11K)$, $(1K1)$	$(11K)$, $(1K\bar{1})$	$(11K)$, $(1K\bar{1})$	$(1\bar{1}K)$, $(1K1)$

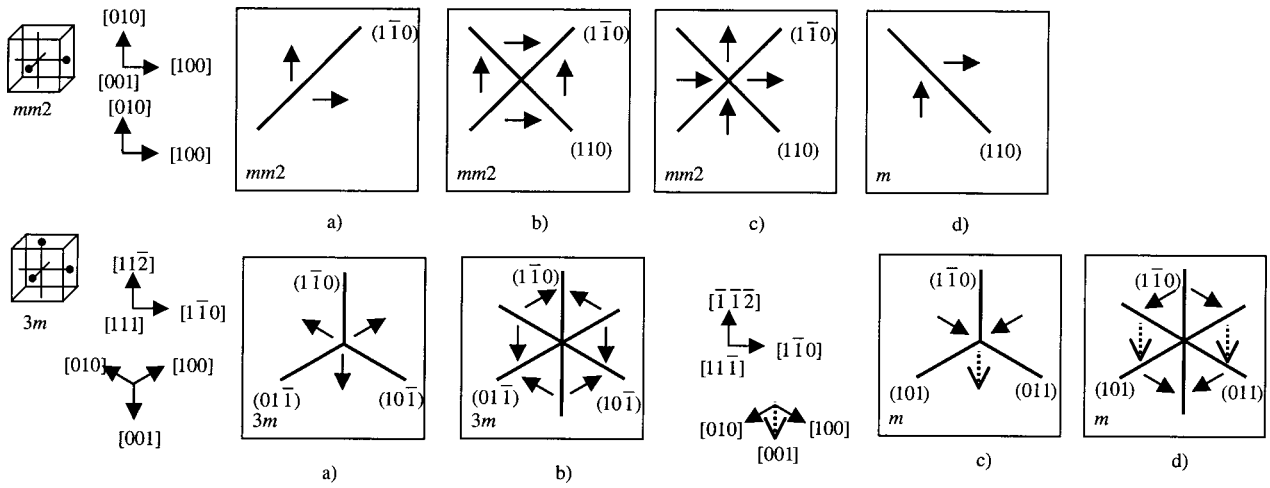

FIG. 2. Multi-domain arrangements with different symmetry descents for $m\bar{3}m \rightarrow 4mm$ ferroelectric species. Domain wall set is plotted by thick lines, orientations of polar directions are marked by arrows (by solid line for arrows pointing up and in the plane in addition to the arrow direction, by dashed line for arrows pointing down the plane in addition to the arrow direction). Polar direction set is schematically displayed by the points on the cube and by the arrows below the coordinate system. Coordinate system axes are plotted at the upper left of the frames, each for one domain configurations. Resulting effective symmetry of the domain structure is labeled in the lower left corner for each configuration.

each given strain state, there are two antiparallel polar directions. These antiparallel states, however, might be present only in an unpoled sample and would be eliminated by electric field poling during the domain engineering process. Therefore, we will not deal with them here to avoid deviating too much from the main objective. All possible domain configurations (without any antiparallel domain pair) are listed in Figs. 2, 3, and 4, respectively, for $m3m \rightarrow 3m$, $m\bar{3}m \rightarrow 4mm$, and $m\bar{3}m \rightarrow mm2$ ferroelectric species. Effective symmetry of domain pattern is determined by the common symmetry elements from both the domain wall set and the polar direction set. The resulting effective symmetry would include this operation only when a symmetry operation in the polar direction set is also an operation in the domain wall set.

Possible symmetry descents found in the domain configurations are summarized in Table VII for $m\bar{3}m \rightarrow 3m$, $m3m \rightarrow 4mm$, and $m\bar{3}m \rightarrow mm2$ ferroelectric species. Most of these structures cannot be used to form domain lattice since they lack two-dimensional translation symmetry. All domain configurations that can fill the whole space in two-dimensional lattice are listed in Table VIII. Their symmetry, piezoelectric properties, and stabilizing electric field and uniaxial mechanical stress directions are specified. Directions for stabilizing fields have been found on the basis of equal degeneracy for all polar directions included in the polar directions set. In many cases, either equally degenerate polar direction set includes more polar directions than in the set under study, or not all the polar directions are energetically degenerate. The last situation is probably the reason for the destabilization of the domain pattern formed after the poling field is removed, as frequently observed in the [111]-poled rhombohedral PZN-PT and PMN-PT crystals. Single domain configuration is observed under strong electric fields (corresponding to [111]-polar direction), but the mixture of domains (corresponding to $[\bar{1}11]$, $[1\bar{1}1]$ and $[11\bar{1}]$ polar directions) is observed after removing the electric field.

Because of the vector nature of the polarization, very few domain configurations, among those domain average symmetries, could have two-dimensional translation symmetry and therefore be stabilized by the poling electric field or uniaxial/biaxial mechanical stresses. As showing in Table VIII, twin or quadruple states can be stabilized for rhombohedral or orthorhombic symmetries, while only twinned domain structure could be stabilized for tetragonal symmetry. If we also include other types of mechanical stress (multi-axial, shear), some other domain configurations might be stabilized, however, practical realization of such fields is rather challenging if not impossible.

III. SUMMARY AND CONCLUSIONS

In summary, we have performed detailed domain symmetry analysis for $m\bar{3}m \rightarrow 3m$, $m\bar{3}m \rightarrow 4mm$, and $m\bar{3}m \rightarrow mm2$ ferroelectric species. Different from previous works of using statistical analysis, we put in all realistic constraints. It is found that only limited configurations are practically realizable, although many possible symmetries were derived using the statistical method. The results reported here can be used as guidance for those who intend to use the domain engineering process to produce property enhanced multi-domain single crystals. For example, there have been attempts to perform the domain-engineering process in [111]-poled tetragonal $BaTiO_3$ crystal;[11] we can predict from our analysis that the intuitive $3m$-symmetry cannot be realized. One can use our symmetry arguments to analyze the experimental data of Ref. 11 and provide sound reasons for the absence of $3m$ symmetry domain structures.

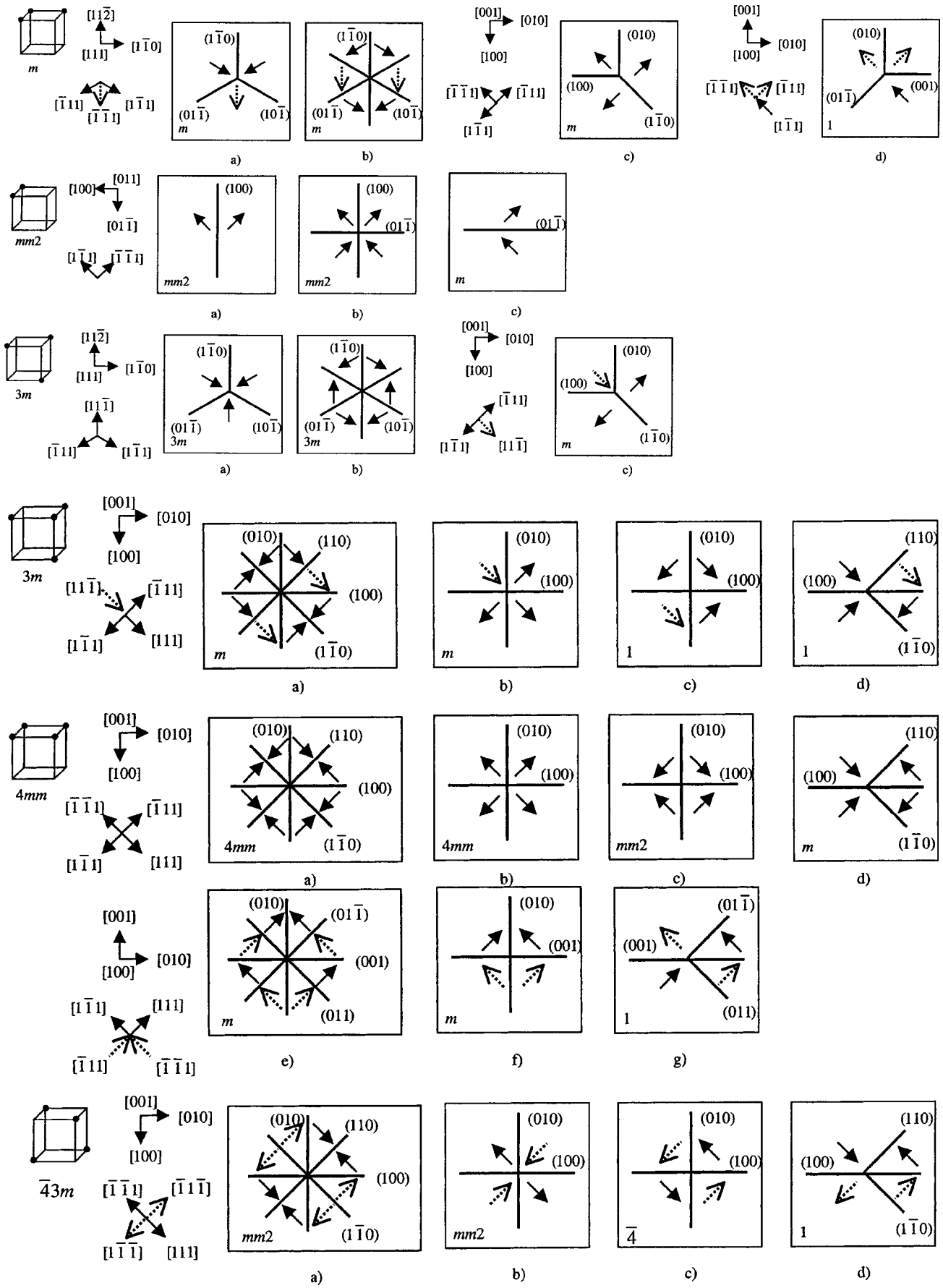

FIG. 3. Multi-domain arrangements with different symmetry descents for $m\bar{3}m \rightarrow 3m$ ferroelectric species. Meaning of arrows and lines is the same as in Fig. 2.

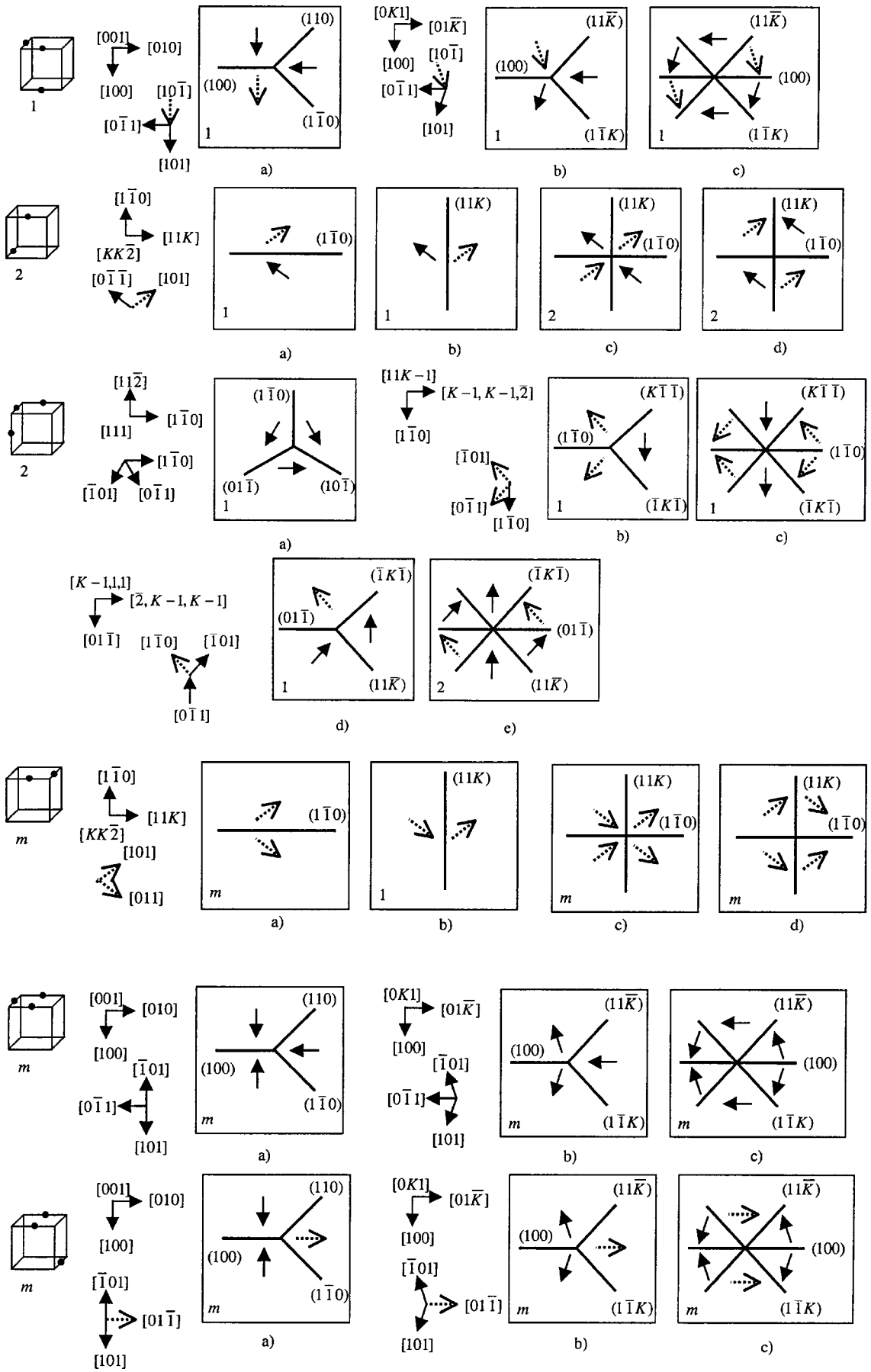

FIG. 4. Multi-domain arrangements with different symmetry descents for $m\bar{3}m \rightarrow mm2$ ferroelectric species. S-wall parameter $K = Q_{44}/Q_{11} - Q_{12}$, value $K = 0.38$ for $BaTiO_3$ is used in figures. Meaning of arrows and lines is the same as in Fig. 2.

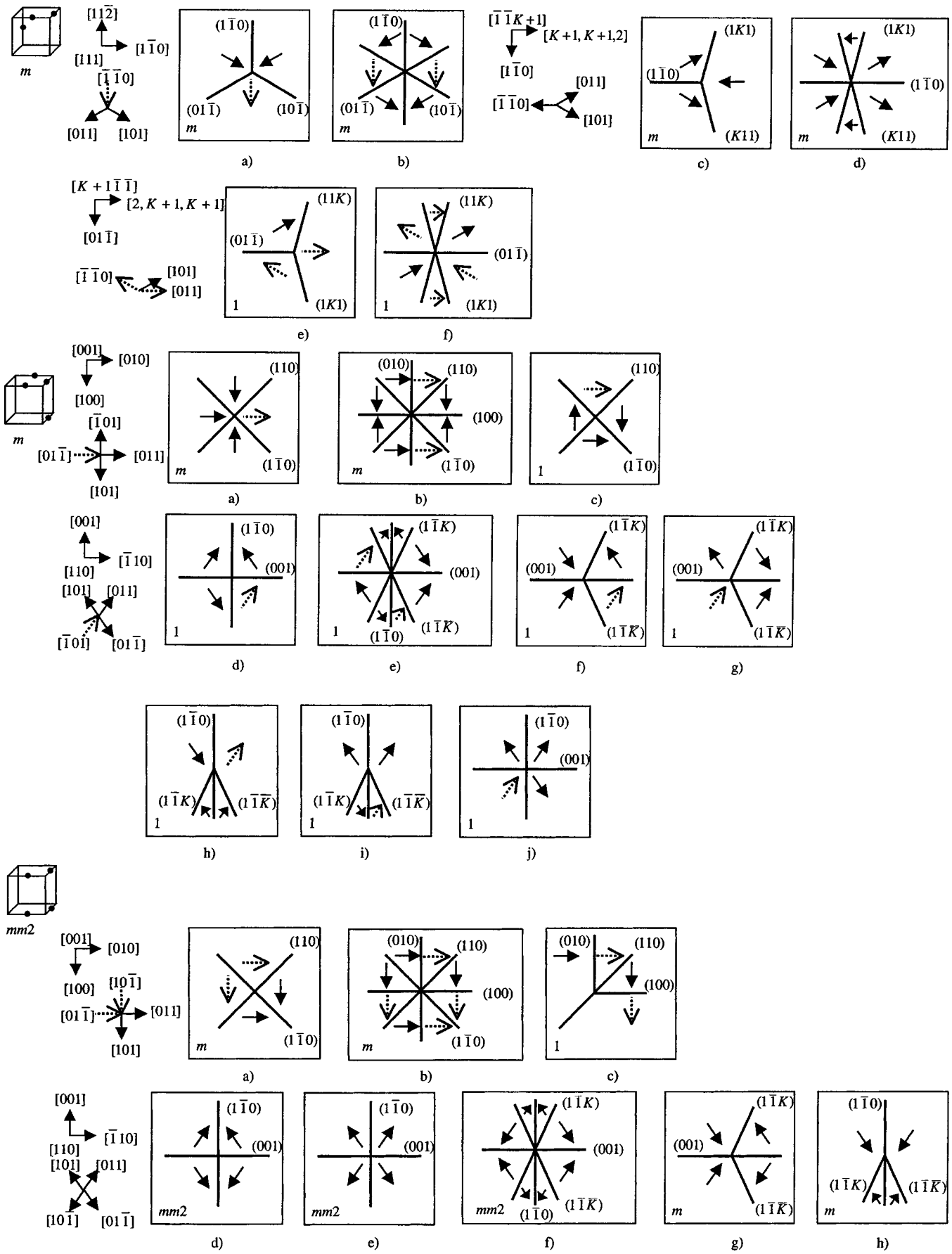

FIG. 4. (*Continued.*)

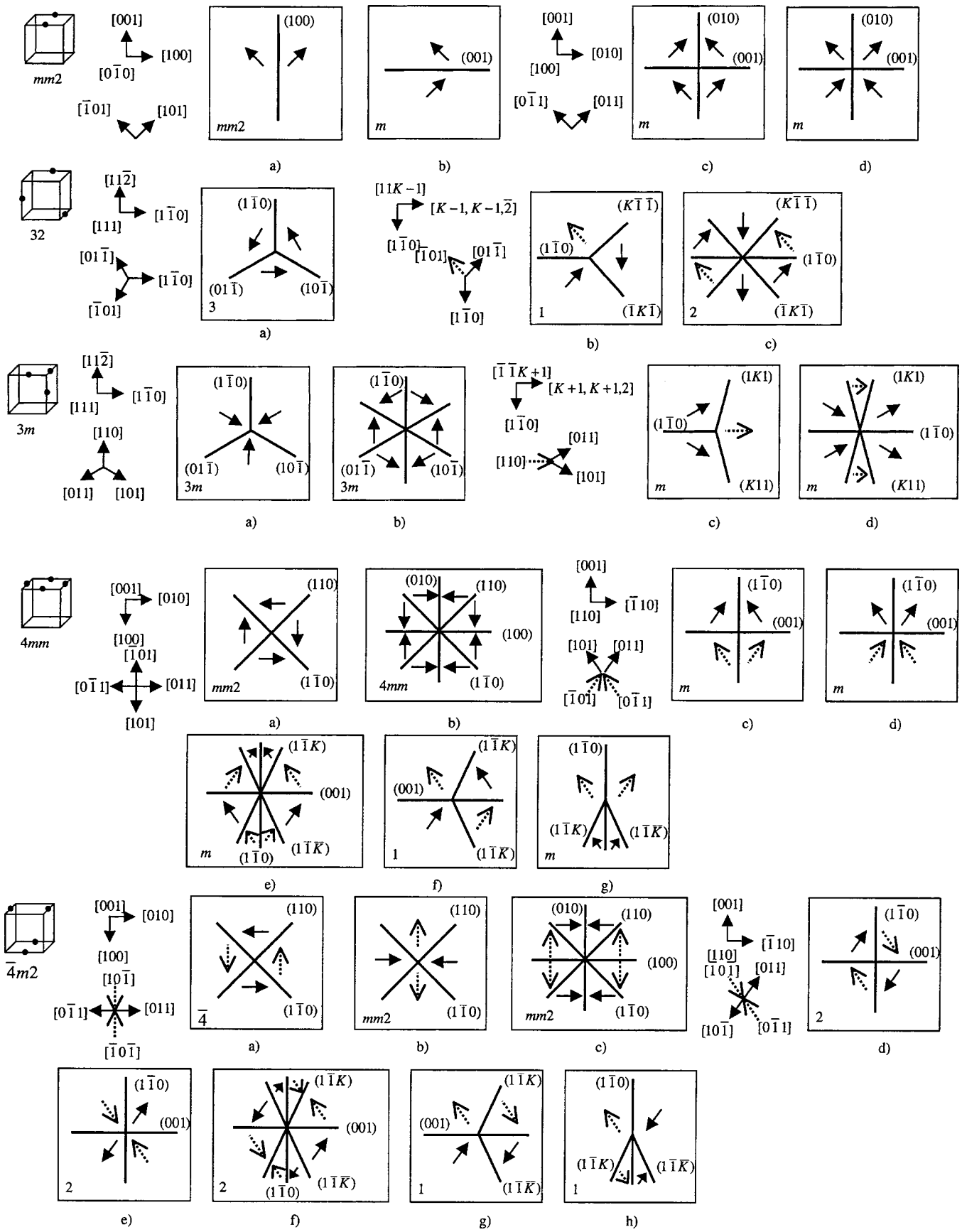

FIG. 4. (*Continued.*)

TABLE VII. Possible symmetry descents in domain configurations for $m\bar{3}m \rightarrow 3m$, $m\bar{3}m \rightarrow 4mm$, and $m\bar{3}m \rightarrow mm2$ ferroelectric species.

Polar direction set's symmetry	Ferroelectric species		
	$m\bar{3}m \rightarrow 3m$	$m\bar{3}m \rightarrow 4mm$	$m\bar{3}m \rightarrow mm2$
1	⋯	⋯	1
2	⋯	⋯	2, 1
m	m, 1	⋯	m, 1
$mm2$	$mm2$, m	$mm2$, m	$mm2$, m
32	⋯	⋯	3, 2, 1
$3m$	$3m$, m, 1	$3m$, m	$3m$, m
$\bar{4}m2$	⋯	⋯	$\bar{4}$, $mm2$, 2, 1
$4mm$	$4mm$, $mm2$, m, 1	⋯	$4mm$, $mm2$, m, 1
$\bar{4}3m$	$mm2$, $\bar{4}$, 1	⋯	⋯

TABLE VIII. Possible domain configurations filling space in two-dimensional lattice for $m\bar{3}m \rightarrow 3m$, $m\bar{3}m \rightarrow 4mm$, and $m\bar{3}m \rightarrow mm2$ ferroelectric species. Stabilizing electric field or uniaxial mechanical stress is parallel to the direction listed. Domain configuration is marked by its effective symmetry and by the number of polar directions involved (in brackets). Different configurations for the same polar direction set are numbered by small letters (a,b,c, ...) corresponding to Figs. 2–4.

Domain configuration		Polar direction set's symmetry	Domain configuration symmetry	Stabilizing electric field	Stabilizing mechanical stress
Ferroelectric species $m\bar{3}m \rightarrow 3m$					
$mm2(2)$	a	$mm2$	$mm2$	$[0\bar{1}1]$	⋯
	b	$mm2$	$mm2$	$[0\bar{1}1]$	
	c	$mm2$	m	$[0\bar{1}1]$	
$3m(4)$	b	$3m$	m	⋯	⋯
	c	$3m$	1		
	d	$3m$	1		
$4mm(4)$	b	$4mm$	$4mm$	[001]	⋯
	c	$4mm$	$mm2$	[001]	
	d	$4mm$	m	[001]	
	f	$4mm$	m	[001]	
	g	$4mm$	1	[001]	
$\bar{4}3m(4)$	b	$\bar{4}3m$	$mm2$	⋯	⋯
	c	$\bar{4}3m$	$\bar{4}$		
	d	$\bar{4}3m$	1		
Ferroelectric species $m\bar{3}m \rightarrow 4mm$					
$mm2(2)$	a	$mm2$	m	[110]	⋯
	b	$mm2$	$mm2$	[110]	
	c	$mm2$	$mm2$	[110]	
	d	$mm2$	$mm2$	[110]	
Ferroelectric species $m\bar{3}m \rightarrow mm2$					
2(2)	a	2	1	⋯	⋯
	b	2	1		
	c	2	2		
	d	2	2		
$m(2)$	a	m	m	[112]	$[11\bar{1}]$
	b	m	1	[112]	$[11\bar{1}]$
	c	m	m	[112]	$[11\bar{1}]$
	d	m	m	[112]	$[111]$

TABLE VIII. (*Continued*).

Domain configuration		Polar direction set's symmetry	Domain configuration symmetry	Stabilizing electric field	Stabilizing mechanical stress
$m(4)$	a	m	m	⋯	⋯
	c	m	1		
	d	m	1		
	f	m	1		
	g	m	1		
	h	m	1		
	i	m	1		
	j	m	1		
$mm2(2)$	a	$mm2$	$mm2$	[001]	[010]
	b	$mm2$	m	[001]	[010]
	c	$mm2$	m	[001]	[010]
	d	$mm2$	m	[001]	[010]
$mm2(4)$	a	$mm2$	m	⋯	⋯
	c	$mm2$	1		
	d	$mm2$	$mm2$		
	e	$mm2$	$mm2$		
	g	$mm2$	m		
	h	$mm2$	m		
$4mm(4)$	a	$4mm$	$mm2$	[001]	⋯
	c	$4mm$	m	[001]	
	d	$4mm$	m	[001]	
	e	$4mm$	m	[001]	
	g	$4mm$	1	[001]	
	h	$4mm$	m	[001]	
$\bar{4}m2(4)$	a	$\bar{4}m2$	$\bar{4}$	⋯	⋯
	b	$\bar{4}m2$	$mm2$		
	d	$\bar{4}m2$	2		
	e	$\bar{4}m2$	2		
	g	$\bar{4}m2$	1		
	h	$\bar{4}m2$	1		

ACKNOWLEDGMENTS

This research is supported by the Hong Kong RGC Grant No. N_CityU114/01. One of the authors (J.E.) is also grateful for the support from the Grant Agency of the Czech Republic under Project No. GACR 202/02/1006.

[1] A. L. Roytburd, S. A. Alpay, L. A. Bendersky, V. Nagarajan, and R. Ramesh, J. Appl. Phys. **89**, 553 (2001).
[2] C. C. Chou and C. S. Chen, Ceram. Int. **26**, 693 (2000).
[3] E. I. Eknadiosiants, V. Z. Borodin, V. G. Smotrakov, V. V. Eremkin, and A. N. Pinskaya, Ferroelectrics **111**, 283 (1990).
[4] J. Yin and W. Cao, J. Appl. Phys. **87**, 7438 (2000).
[5] J. K. Lee, J. Y. Yi, K. S. Hong, S. E. Park, and J. Milan, J. Appl. Phys. **91**, 4474 (2002).
[6] F. Jona and G. Shirane, *Ferroelectric Crystals* (Dover, New York, 1993), Fig. IV-42 on p. 169.
[7] E. Wiesendanger, Czech. J. Phys., Sect. B **23**, 91 (1973).
[8] Li Lian, T. C. Chong, H. Kumagai, M. Hirano, Lu Taijing, and S. C. Ng, J. Appl. Phys. **80**, 326 (1996).
[9] S. E. Park and T. R. Shrout, J. Appl. Phys. **82**, 1804 (1997).
[10] S. E. Park, S. Wada, L. E. Cross, and T. R. Shrout, J. Appl. Phys. **86**, 2746 (1999).
[11] S. Wada, S. Suzuki, T. Noma, T. Suzuki, M. Osada, M. Kakihana, S. E. Park, L. E. Cross, and T. R. Shrout, Jpn. J. Appl. Phys., Part 1 **38**, 5505 (1999).
[12] S. Wada, A. Seike, and T. Tsurumi, Jpn. J. Appl. Phys., Part 1 **40**, 5690 (2001).

[13] Y.-M. Chiang, G. W. Farrey, and A. N. Soukhojak, Appl. Phys. Lett. **73**, 3683 (1998).
[14] S. Zhang, P. W. Rehrig, C. Randall, and T. R. Shrout, J. Cryst. Growth **234**, 415 (2002).
[15] S. Zhang, S. Rhee, C. A. Randall, and T. R. Shrout, Jpn. J. Appl. Phys., Part 1 **41**, 722 (2002).
[16] J. Fousek, D. B. Litvin, and L. E. Cross, J. Phys.: Condens. Matter **13**, L33 (2001).
[17] D. Hatch, H. T. Stokes, and W. Cao (unpublished).
[18] J. Fuksa and V. Janovec, J. Phys.: Condens. Matter **14**, 3795 (2002).
[19] J. Erhart and W. Cao, J. Mater. Res. **16**, 570 (2001).
[20] J. Yin, B. Jiang, and W. Cao, IEEE Trans. Ultrason. Ferroelectr. Freq. Control **47**, 285 (2000).
[21] R. Zhang, B. Jiang, and W. Cao, J. Appl. Phys. **90**, 3471 (2001).
[22] J. Yin and W. Cao, J. Appl. Phys. **92**, 444 (2002).
[23] J. Fousek and V. Janovec, J. Appl. Phys. **40**, 135 (1969).